Bull. Mater. Sci., Vol. 37, No. 3, May 2014, pp. 497–504. © Indian Academy of Sciences.

Magnetodielectric effect in $Ni_{0.5}Zn_{0.5}Fe_2O_4$–$BaTiO_3$ nanocomposites

SHILPI BANERJEE[1,2], PARTHA HAJRA[1], ANINDYA DATTA[3], ASIM BHAUMIK[2], MYKANTH REDDY MADA[4], SRI BANDYOPADHYAY[4] and DIPANKAR CHAKRAVORTY[1,*]

[1]MLS Professor's Unit, Indian Association for the Cultivation of Science, Kolkata 700032, India
[2]Department of Materials Science, Indian Association for the Cultivation of Science, Kolkata 700 032, India
[3]University School of Basic and Applied Science (USBAS), Guru Govind Singh Indraprastha University, New Delhi, India
[4]School of Materials Science and Engineering, University of New South Wales, Kensington, Sydney-2052, Australia

MS received 6 March 2013; revised 3 June 2013

Abstract. Composites comprising of nanoparticles of $Ni_{0.5}Zn_{0.5}Fe_2O_4$ (NZF) and $BaTiO_3$ (BT), respectively were synthesized by a chemical method. The particles had diameters in the range of 15–31 nm. NZF was prepared by a coprecipitation technique. This was soaked in a sol containing BT. Compositions synthesized were xNZF-$(1-x)$ BT, where x = 0·7, 0·5 and 0·3, respectively. The composites showed ferromagnetic hysteresis loops due to NZF phase. The analysis of coercivity variation as a function of temperature gave blocking temperatures in the range of 306–384 K depending on the diameter of the ferrite nanoparticles. This implied that superparamagnetic interactions are above these temperatures. The nanocomposites also exhibited ferroelectric behaviour arising due to the presence of BT. The remanent polarization of the samples was small. This was adduced to the nanosize of BT. The specimens showed magneto-dielectric (MD) effect in the magnetic field range 0–0·7 Tesla. The MD parameter measured at the maximum magnetic field was around 2%. This was one order of magnitude higher than that reported so far in similar composite systems. This was explained on the basis of a two-phase inhomogeneous medium model with an interface between them, the phases possessing drastically different electrical conductivities.

Keywords. Nanocomposites; magneto-dielectric effect; two-phase inhomogeneous medium; Maxwell–Wagner effect.

1. Introduction

Intense research on multiferroic materials in recent years has been driven both by basic physics considerations as well as technological prospects (Filipetti and Hill 2001; Kuroiwa *et al* 2001; Fiebig *et al* 2002, 2006; Fiebig 2005; Spaldin and Fiebig 2005; Catalan 2006; Eerenstein *et al* 2006; Argyriou *et al* 2007). These materials exhibit both ferroelectric and ferromagnetic order (Jiang *et al* 2006). Thus, they can be used in multifunctional devices. Also, the magnetoelectric coupling shown by the multiferroic materials make them ideally suited for the use as magnetic field sensors. Such systems however, are rare in nature. These single phase materials show low values of magnetoelectric coupling coefficient making it difficult to fabricate suitable device out of them. This has necessitated research on development of composite multiferroic systems combining suitable ferromagnetic and ferroelectric materials with a morphology, which will ensure good mechanical coupling between the two phases caused by the magnetostrictive property of the ferromagnetic phase. Such a mechanical strain brings about a dielectric polarization change in the ferroelectric phase due to piezoelectric effect. A number of studies were carried out on composite structures (Kadam *et al* 2003; Srinivasan *et al* 2003; Zhai *et al* 2004; Tan *et al* 2008; Liu *et al* 2010; Jiang *et al* 2011). The components were various ferrites on the one hand and barium titanate or lead zirconate titanate (PZT) on the other. Core–shell particulate composites were also investigated (Corral-Flores *et al* 2006, 2010; Duong *et al* 2006; Raidongia *et al* 2010). In the latter, a ferrite phase formed the core and barium titanate the shell. Besides these, both multilayer (Srinivasan *et al* 2003; Zheng *et al* 2004) and laminate (Nersessian *et al* 2003; Dong *et al* 2004) configurations have also been studied. In these investigations, the ferromagnetic phase was a ferrite, e.g. $MgFe_2O_4$, $CoFe_2O_4$, etc. There are a number of studies reported in recent times on composites consisting of nickel zinc ferrite and barium titanate (Testino *et al* 2006; Harnagea *et al* 2007; Devan *et al* 2008; Sreenivasalu *et al* 2009; Zhang *et al* 2009; Shen *et al* 2010). The composites were synthesized by either a co-precipitation route or by a direct mixing of the nanosized powders of the two phases concerned. The coupling between the magnetic and electric ordering in

*Author for correspondence (mlsdc@iacs.res.in)

such nanocomposites has not led to a significant value of magnetoelectric coupling coefficient. This is believed to be due to rather low values of effective magnetic field on the ions in the ferroelectric phase or low effective electric field on the ions in the magnetic phase due to the dipoles in the ferroelectric nanophase. Recent theoretical investigation has shown that a magnetodielectric effect can be induced in a system containing interfaces between two phases having drastically different electrical conductivities. Maxwell–Wagner polarization at the latter combined with Hall effect, then leads to a lowering of the dielectric constant of the composite, when subjected to a magnetic field (Catalan 2006; Parish and Littlewood 2008). Our motivation was therefore to exploit the low resistivity of nickel zinc ferrite to form a Maxwell–Wagner interface with high resistivity barium titanate such that a reasonably large value of magnetodielectric coefficient could be achieved in the nanocomposite system. The composite samples were prepared by a chemical method. Magnetic, dielectric and magneto-dielectric properties were studied. Indeed, a rather high value of magneto dielectric (MD) parameter was obtained in these composite samples. The dielectric loss was however, low, making them suitable for practical applications. The details are reported in this paper.

2. Experimental

$Ni_{0.5}Zn_{0.5}Fe_2O_4$ was synthesized by a chemical co-precipitation method. Stoichiometric amounts of $NiCl_2{\cdot}6H_2O$, $ZnCl_2$ and $FeCl_3$ (the latter two were anhydrous) were dissolved in distilled water with constant stirring. The pH of the solution was maintained in the range of 12–14 by adding suitable amount of sodium hydroxide solution. The chemical reaction was carried out at 358 K for a duration of 45 min. The NZF precipitate was thoroughly washed with distilled water to free it from sodium and chlorine ions. The product was dried at a temperature of 333 K for one week. The resultant powder was homogenized by using an agate mortar and pestle. In the next step, a sol containing barium titanate was prepared. For this, a solution was made by mixing ethyl alcohol and acetic acid in volume ratio of 3 : 1. Tetraisopropylorthotitanate ($C_{12}H_{28}O_4Ti$) was then added to the above solution with a volume ratio of 1 : 20 with acetic acid. The mixture was stirred for 2 h. Another solution was made by dissolving barium acetate in distilled water such that the molar ratio of Ba to Ti (in the other solution) was 1 : 1. The solution was stirred for half an hour. The latter was poured into the first solution and the mixture was stirred for one hour. Ferrite powder prepared as described previously was soaked in this solution in three proportions, viz. 70, 50 and 30 mol% (denoted in subsequent discussions as A, B and C, respectively). The mixtures were separately stirred for 20 h. The resultant gels were dried at room temperature for one week.

Differential thermal analysis (DTA) of the gel was carried out in a TA Instrument (SDT Q600). A crystallization temperature for the growth of $BaTiO_3$ phase was determined from such analysis. The temperature was found to be 973 K. Accordingly, the dried gel prepared as above was subjected to a heat treatment at 973 K for 6 h. X-ray diffraction of different samples was done by X-ray diffractometer model Bruker D8 using CuKα radiation. The microstructures of the samples were studied by a JEOL 2010 transmission electron microscope. Magnetic properties were investigated by an MPMS superconducting quantum interference device magnetometer (supplied by M/s Quantum Design, USA). The temperature range of measurement was 2–300 K. For dielectric property studies, pellet specimens were prepared by taking the powder in a mould of 1 cm diameter and then subjecting the same to cold pressing with a load of 5 tons. Typical sample thickness was 0·5 mm. The pellet was sintered at 1173 K for 3 h. Silver paste (supplied by M/s Acheson Colloiden, Netherlands) was used to paint both surfaces of the specimen, which were used as electrodes. Ferroelectric behaviour at room temperature was investigated using an automatic P–E loop tracer manufactured by M/s Marine India Electricals Private Ltd. For magnetodielectric property studies, the samples were placed between the pole pieces of an electromagnet supplied by M/s Control Systems and Devices, Mumbai, India. The capacitance change as a function of applied magnetic field was measured using an Agilent E4890A precision LCR meter at a frequency 400 kHz.

3. Results and discussion

Figure 1 shows X-ray diffractograms obtained from different samples prepared. The diffraction peaks have been identified with the lattice planes of $Ni_{0.5}Zn_{0.5}Fe_2O_4$ and $BaTiO_3$ phases, respectively, and are indicated by the corresponding Miller indices in the figure. There are a few small peaks which have been identified to correspond to the phase α-Fe_2O_3. The latter being antiferromagnetic, does not contribute to the magnetic properties of the composite as described below. The presence of α-Fe_2O_3 phase in samples A and B acts as a bulwark against a percolative configuration of $Ni_{0.5}Zn_{0.5}Fe_2O_4$, which has a high electrical conductivity. This is beneficial because it ensures a low value of dielectric loss ($\tan\delta$), which is necessary from the point of view of practical application. The results and discussion in later sections will bear this out. It is to be noted that figures 1(b) and (c) give Miller indices for planes in $Ni_{0.5}Zn_{0.5}Fe_2O_4$ and $BaTiO_3$, respectively. It can be seen from figures 1(a) and (c), respectively, that the intensities of the diffraction peaks for $BaTiO_3$ decrease as its content decreases and those for $Ni_{0.5}Zn_{0.5}Fe_2O_4$ increase as one goes from sample C to A. This is consistent with the sample composition as delineated in

Table 1. Summary of crystallite sizes in different specimens.

	Specimen A (nm)	Specimen B (nm)	Specimen C (nm)
BT	22·9	31·6	34·6
NZF	23·0	27·9	35·1

Table 2. Comparison of d_{hkl} values obtained from electron diffraction rings from figure 2(b) with ASTM data.

Observed d_{hkl} (nm)	ASTM data of $Ni_{0.5}Zn_{0.5}Fe_2O_4$ (JCPDS no. 08-0234) (nm)	ASTM data of $BaTiO_3$ (JCPDS no. 05-0626) (nm)	Corresponding miller indices (*hkl*)
0·301	0·2966		(220)
0·283		0·2838	(101)
0·251	0·2533		(311)
0·212	0·2110		(400)
0·163		0·1634	(211)
0·150	0·1485		(440)

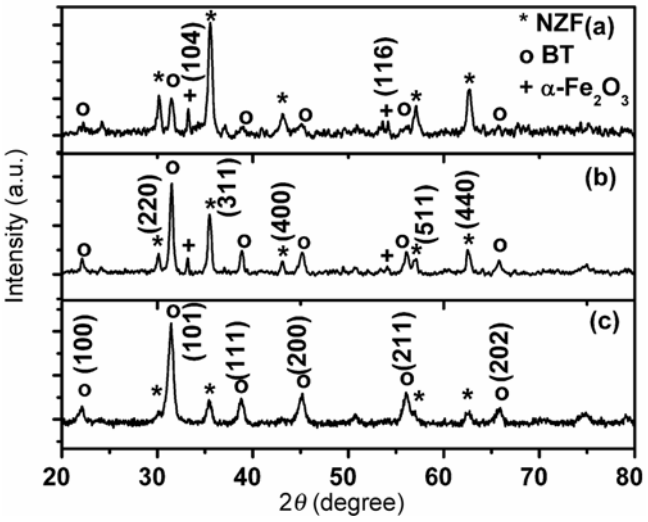

Figure 1. X-ray diffractograms of different specimens: (**a**) specimen A, (**b**) specimen B and (**c**) specimen C.

the preparation procedure. The crystallite sizes of the phases were estimated using Scherrer's formula (Cullity 1978). These are summarized in table 1.

Figure 2(a) gives the electron micrograph of specimen A. This is typical of the microstructure observed in other specimens also. Figure 2(b) is the selected area of electron diffraction pattern obtained from figure 2(a). The interplanar spacings d_{hkl} were calculated from the diameters of the rings along which diffraction spots were found. Table 2, summarizes the results. The Miller indices of the planes are also shown in a separate column. It can be seen that both $Ni_{0.5}Zn_{0.5}Fe_2O_4$ and $BaTiO_3$ phases are present in our samples. Figure 3 shows the high resolution transmission electron micrograph of specimen A. The planes (311) of $Ni_{0.5}Zn_{0.5}Fe_2O_4$ are indicated. Also we see the planes (101) of $BaTiO_3$ phase. The FFT of figure 3 is shown in the inset. For calculating the mean particle diameters in different samples, the particle size histogram as found from micrograph such as figure 2(a) was plotted and the data fitted to a lognormal distribution function. The extracted values of median diameter are shown in the second column of table 3. It should be noted that the median diameters refer to particles of both the phases. It must be pointed out that our sample system is a composite of two nanocrystalline phases, viz. $Ni_{0.5}Zn_{0.5}Fe_2O_4$ and $BaTiO_3$, respectively, forming interfaces with each other. They do not form a core–shell structure. This should be evident from figure 3, in which the interface between two nearest neighbouring NZF and BT nanoparticles can be seen.

After characterization of the microstructures delineated as above, we now discuss the effects of these on the magnetic, dielectric and magneto-dielectric properties of different samples studied here. In figures 4(a–c) are shown the magnetic hysteresis of the three samples at room temperature, 100 and 2 K, respectively. This is typical of the hysteresis behaviour at other temperatures. The coercivities of the samples were extracted from the hysteresis loops. Figures 5(a–c) give the variation of coercivity, H_c as a function of temperature for specimens A, B and C, respectively. It is seen that the coercivity increases as the temperature is reduced. It has been shown that for an assembly of ferromagnetic nanoparticles, the variation of H_c as a function of temperature is given by (Childress *et al* 1990; Martinez *et al* 1996):

$$H_c = H_{co}\left[1-\left(\frac{T}{T_B}\right)^{1/2}\right], \tag{1}$$

where H_{co} is a constant related to the saturation magnetization and the volume magneto-crystalline anisotropy and T_B the blocking temperature. H_{co} was determined by extrapolation of the curves in figure 5 to $T = 0$ K. The

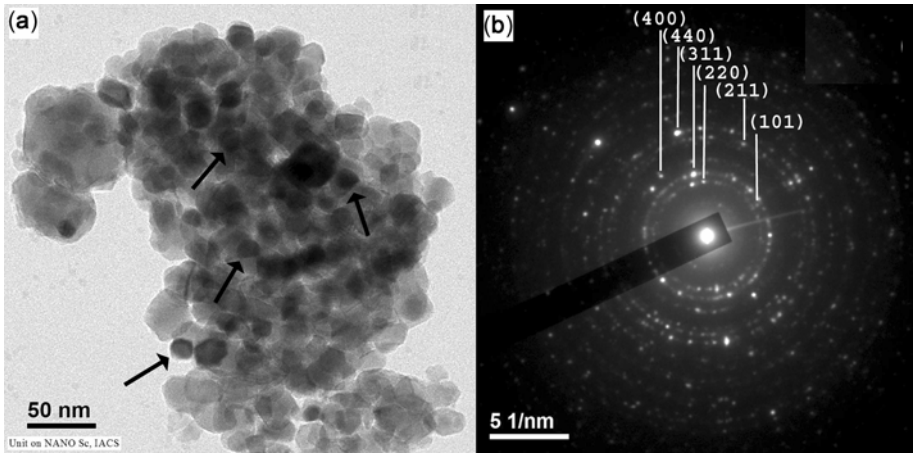

Figure 2. (**a**) Transmission electron micrograph of specimen A and (**b**) selected area electron diffraction patterns obtained from figure 2(a).

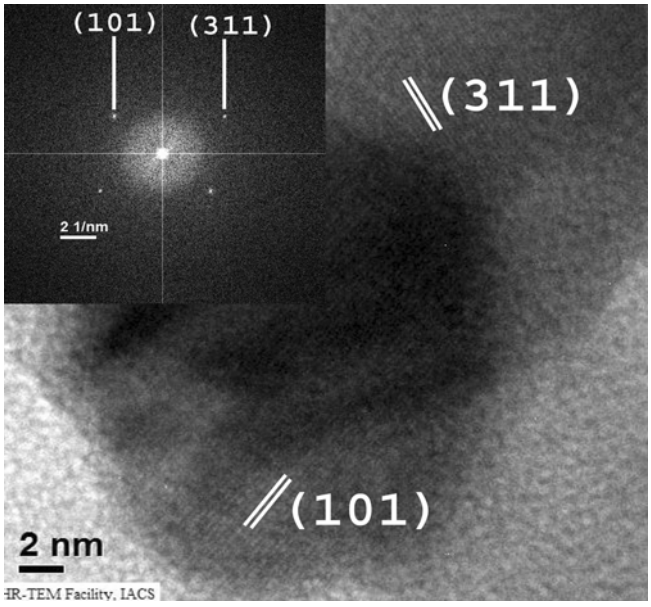

Figure 3. High resolution transmission electron micrograph of figure 2(a).

intersection of the curves with the ordinate gave H_{co} values. Using the latter, the experimental data given in figures 5(a–c) were fitted to (1) and the theoretical points are also shown in these figures. The extracted value of T_B is given by (Childress *et al* 1990; Martinez *et al* 1996):

$$T_B = \frac{KV}{25k}, \tag{2}$$

where K is the anisotropy energy density, V the volume of the particle and k is Boltzmann's constant. The volume of the particle was calculated from the relation:

$$V = \frac{\pi d^3}{6}, \tag{3}$$

where d is the particle diameter. Substituting the values of T_B for different specimens and the corresponding particle diameters, we have calculated their anisotropy energy density values. These are shown in the last column of table 3. The values are almost two orders of magnitude higher than that for bulk $NiFe_2O_4$ ($\sim 6{\cdot}2 \times 10^3$ erg/cc) (Galt *et al* 1950; Yager *et al* 1951). It is evident that the magnetocrystalline anisotropy increases as the particle size is reduced. This is consistent with our earlier studies in a related system (Pal *et al* 1996). We would like to point out here, that T_B can in principle, be directly determined from the zero field cooled and field cooled magnetization data as a function of temperature. The temperature at which these two curves merge corresponds to T_B. There are however problems to find this especially, when T_B has a value greater than room temperature and the desired point is difficult to delineate. The procedure outlined above has been used earlier to find the values of T_B as well as K (Banerjee *et al* 2012, 2013).

Figure 6(a) gives a polarization-electric field hysteresis curve obtained in the case of sample B confirming the presence of ferroelectric behaviour. This is typical of all the samples studied. The remanent polarization obtained is 0·05 μC/cm^2, which is rather small. This could be due to small particle size of the $BaTiO_3$ (Uchino *et al* 1989; Zhong *et al* 1994; Zhao *et al* 2004) phase in our samples. However, the saturation of polarization is indicated in figure 6(a) by the extrapolated dotted lines as shown. Figures 6(b) and (c) show P–E hysteresis loop for samples C and A, respectively.

In figures 7(a–c) are shown the variation of dielectric constant as a function of applied magnetic field for the three specimens A, B and C, respectively, measured at a frequency of 400 kHz. It is seen that the dielectric constant decreases as the $BaTiO_3$ content in the composite is reduced. This is to be expected. For explaining the variation of dielectric constant as a function of applied magnetic

Table 3. Extracted values of H_{co} and T_B for different nanocomposites.

Specimen	Particle diameter (nm)	Volume V $(nm)^3$	H_{CO} (Oe)	T_B (K)	K (erg/cc)
A	15	1766·2	209·4	305·9	$5{\cdot}9 \times 10^5$
B	23·1	6450·7	234·5	381·8	$2{\cdot}1 \times 10^5$
C	31·2	15894·3	280·5	384·1	$0{\cdot}8 \times 10^5$

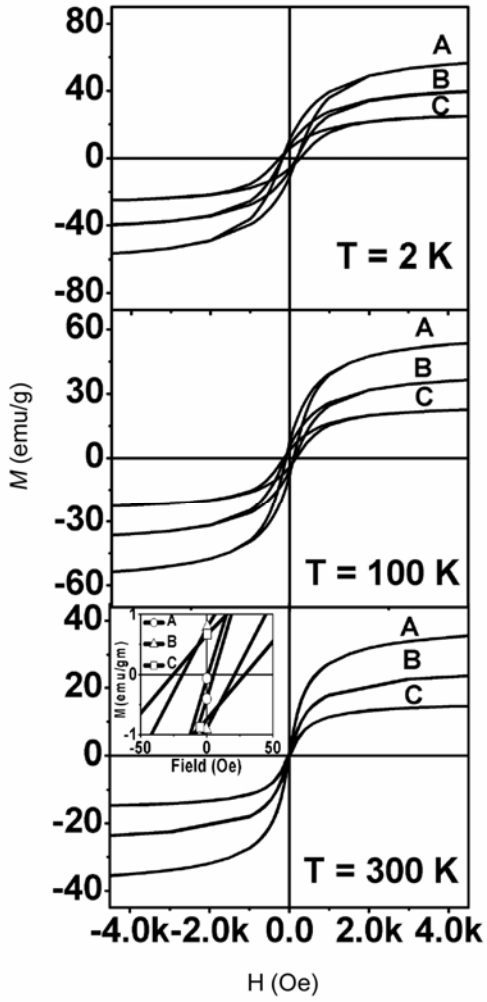

Figure 4. Magnetic hysteresis loops for different specimens.

field, we introduced the model of a two-phase inhomogeneous medium reported recently (Parish *et al* 2008). According to this model, in a composite medium consisting of two phases having different conductivities and an interface between them Maxwell–Wagner polarization causes a magnetocapacitance effect without multiferroicity. An electric field applied for measuring dielectric constant will cause electric current flow through the phase with higher conductivity and give rise to space charges at the interface. Application of a magnetic field will cause Hall effect to be operative deflecting some of the charges in a perpendicular direction, thereby reducing the accumulated charge at the interface. This, in turn will lower the value of dielectric constant of the composite. We had carried out resistivity measurements at room temperature for a pellet sample made up of $Ni_{0.5}Zn_{0.5}Fe_2O_4$ nanoparticles of diameter 14 nm, cold compacted and sintered at 573 K for 15 min. Also the resistivity of samples A, B and C were measured. These values are summarized in table 4.

It can be seen that $Ni_{0.5}Zn_{0.5}Fe_2O_4$ has a resistivity around $4{\cdot}1 \times 10^6$ ohm-cm which is almost two orders of magnitude less than the composites. Hence, space-charge polarization of Maxwell–Wagner type will be effective in our system and a magnetic field will reduce the dielectric constant of the sample. The interfaces between the $Ni_{0.5}Zn_{0.5}Fe_2O_4$ and $BaTiO_3$ phases give rise to space charge accumulation. From figure 2(a), it can be seen that there are regions where the two phases have a two-dimensional configuration and overlap each other (shown by arrows). Considering the fact that the NZF and BT phases have crystallite sizes of almost the same magnitude (see table 1), it should be possible to use the equation for the effective dielectric permittivity (Parish *et al* 2008) which is given by:

$$\bar{\varepsilon} = \varepsilon \frac{(1+iw\tau)}{\sqrt{iw\tau}\sqrt{(1+iw\tau)^2 - (w\tau\beta)^2}}, \tag{4}$$

where $\bar{\varepsilon}$ is the effective dielectric constant, w the angular frequency of the applied electric field, ε the dielectric constant of the barium titanate phase $\tau = \rho\varepsilon$, ρ being the resistivity of the conducting phase (ferrite), $\rho = \mu$H, μ being the carrier mobility of the conducting phase and H is the applied magnetic field. It should be mentioned here that in our system a small amount of α-Fe_2O_3 is also present. It should be stressed here that the regions in the sample contributing to the Maxwell–Wagner and Hall effect satisfy the conditions under which (4) was derived. In fact, this equation was used earlier in a different nanocomposite system (Mandal *et al* 2012) under similar circumstances.

The experimental data were fitted to (4) using μ as the parameter. The theoretically fitted values are also shown in figures 7(a–c). The experimental points match the theoretical values satisfactorily. We have estimated the μ value from the concentration of carriers (in this case small polarons) as calculated using the number of iron ions per molecule of $Ni_{0.5}Zn_{0.5}Fe_2O_4$ (Gul *et al* 2008).

Table 4. Room temperature resistivities of $Ni_{0.5}Zn_{0.5}Fe_2O_4$ and $Ni_{0.5}Zn_{0.5}Fe_2O_4$–$BaTiO_3$ nanocomposites.

	Mobility (cm^2/V-s)			
Specimen	Dielectric loss (tanδ)	Resistivity (ohm-cm)	Estimated from resistivity	Extracted by fitting of (4)
$Ni_{0.5}Zn_{0.5}Fe_2O_4$ (nanoparticle diameter 14 nm)		$4{\cdot}1 \times 10^6$	$1{\cdot}05 \times 10^{-10}$	
A	0·301	$1{\cdot}66 \times 10^8$		$3{\cdot}63 \times 10^{-10}$
B	0·174	$3{\cdot}89 \times 10^8$		$1{\cdot}46 \times 10^{-10}$
C	0·151	$2{\cdot}78 \times 10^9$		$3{\cdot}59 \times 10^{-10}$

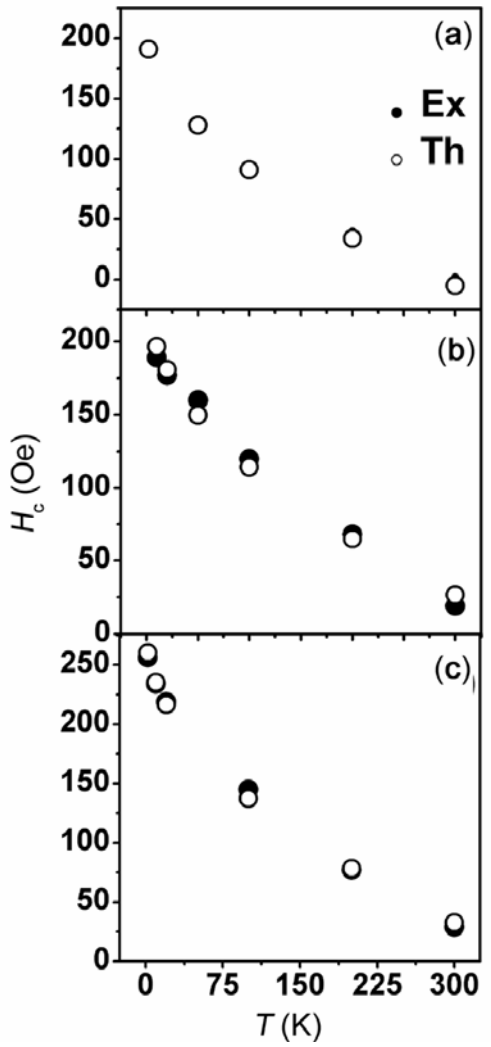

Figure 5. Variation of coercivity, H_C as a function of temperature for different specimens: (**a**) specimen A, (**b**) specimen B and (**c**) specimen C.

These are given in the third column of table 4. It is found to have a value, which is of the same order of magnitude as that extracted from the theoretical fitting described above. The second column in table 4 gives the measured values of dielectric loss (tan δ) at a frequency 400 kHz.

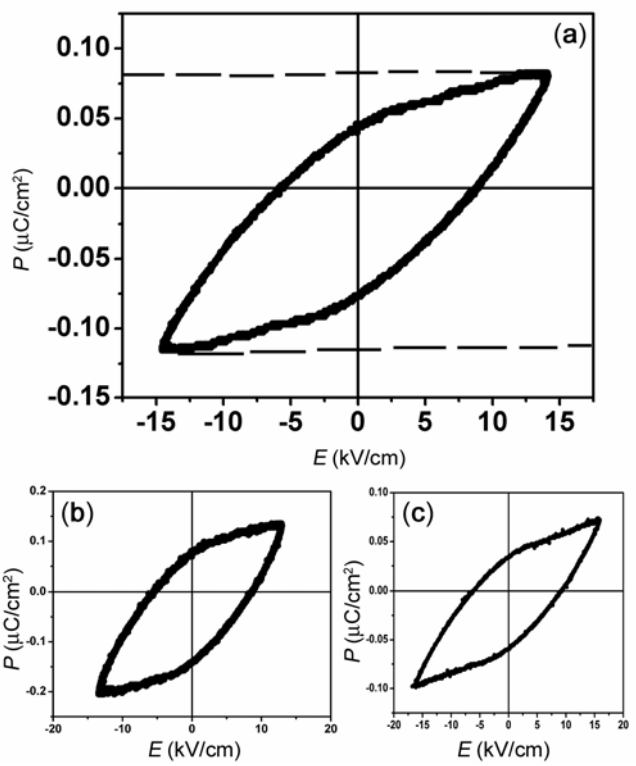

Figure 6. Polarization vs electric field hysteresis curve of (**a**) specimen B, (**b**) specimen C and (**c**) specimen A.

We have summarized the magnetodielectric (MD) effect as shown by these data in figure 8, where the percentage variation of MD defined as $[\varepsilon(H) - \varepsilon(0)]/\varepsilon(0)$ is shown as a function of applied magnetic field. $\varepsilon(H)$ and $\varepsilon(0)$ being the dielectric constants corresponding to magnetic fields H and zero, respectively. It can be seen that the values are in the range of 1·2–2% at a magnetic field of 0·7 Tesla. These values are an order of magnitude higher than those reported earlier in a composite system $MgFe_2O_4$–$BaTiO_3$ (Tan *et al* 2008). We conclude that by proper manipulation of the nanostructure in a suitably chosen system, a high value of magnetodielectric (MD) parameter can be achieved, which is caused not by multiferroicity, but by Maxwell–Wagner space charge at the interface and the effect of magnetic field thereon.

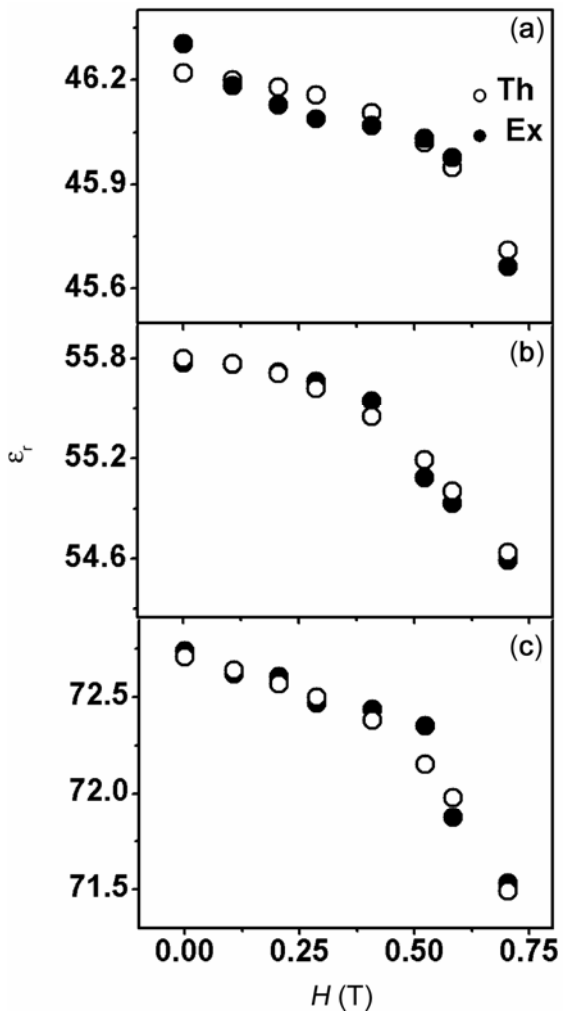

Figure 7. Variation of dielectric constant as a function of applied magnetic field for different specimens at a frequency of 400 kHz with theoretically fitted data: (**a**) specimen A, (**b**) specimen B and (**c**) specimen C.

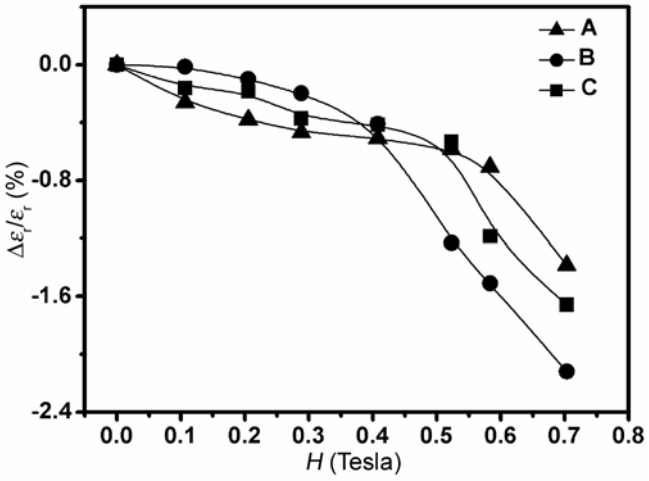

Figure 8. Variation of MD% as a function of applied magnetic field for different specimens.

From the results and discussions described in the previous paragraphs, we can correlate the different properties measured with the nanostructures of our samples as follows.

The nanocomposites comprised of nanoparticles of $Ni_{0.5}Zn_{0.5}Fe_2O_4$ and $BaTiO_3$ forming interfaces between them with a very small amount of α-Fe_2O_3 also present. The ferrite particles exhibited ferromagnetic hyteresis with the coercivity increasing as the temperature was lowered. This has been shown to be consistent with the theory of magnetic behaviour of an assembly of ferromagnetic nanoparticles. Using this model, the blocking temperatures were estimated for different particle sizes. The anisotropy energy density values for these particles were also calculated, which were much larger than that for bulk ferrite samples. A ferroelectric hysteresis was found in our nanocomposites, which showed a rather low value of remanent polarization. This was ascribed to the nanometre size of the $BaTiO_3$ phase present in the system.

The nanostructure of these composites with the electrically conducting $Ni_{0.5}Zn_{0.5}Fe_2O_4$ particles forming interfaces with the highly-insulating $BaTiO_3$ particles formed an ideal system to generate space charge polarization. The effect of magnetic field on these charges was to cause a change in the dielectric constant of the composite. This behaviour was indeed observed and studied using the model of Parish and Littlewood (2008) in our system.

4. Conclusions

Composites comprising nanoparticles of $Ni_{0.5}Zn_{0.5}Fe_2O_4$ and $BaTiO_3$, respectively, having diameters in the range of 15–31 nm were prepared by a chemical method. The nanocomposites exhibited ferromagnetic hysteresis due to NZF phase. Blocking temperatures in the range of 306–384 K were deduced from the coercivity data implying superparamagnetic interaction among the NZF nanoparticles above these temperatures. The samples also showed ferroelectric behaviour due to BT phase with small remanent polarization because of a nanosize effect. The specimens exhibited magneto–dielectric effect with an MD parameter of around 2% at a magnetic field of 0·7 Tesla. This is an order of magnitude higher than that reported earlier in similar systems. This behaviour was explained on the basis of a two-phase inhomogeneous medium model with an interface between the two phases having drastically different conductivities.

Acknowledgement

The research was supported by the Department of Science and Technology (DST), Govt. of India, New Delhi, under an Indo-Australian project on nanocomposites. (SB) thanks CSIR, New Delhi, for the award of a Senior

Research Fellowship. (DC) thanks the Indian National Science Academy, New Delhi, for awarding him an Honorary Scientist's position. The authors thank Sreemanta Mitra for his help with some of the computations.

References

Argyriou D N, Aliouane N, Strempfer J, Zegkinoglou I, Bohnenbuck B, Habicht K and Zimmermann M V 2007 *Phys. Rev.* **B75** 020101

Banerjee S, Bhunia M K, Bhaumik A and Chakravorty D 2012 *J. Appl. Phys.* **111** 054310

Banerjee S, Hajra P, Mada M R, Bhaumik A, Bandyopadhyay S and Chakravorty D 2013 *J. Magn. Magn. Mater.* **332** 98

Catalan G 2006 *Appl. Phys. Lett.* **88** 102902

Childress J R, Chien C L and Nathan M 1990 *Appl. Phys. Lett.* **56** 95

Corral-Flores V, Bueno-Baques D, Carrillo-Flores D and Matutes-Aquino J A 2006 *J. Appl. Phys.* **99** 08J503

Corral-Flores V, Bueno-Baqués D and Ziolo R F 2010 *Acta Mater.* **58** 764

Cullity B D 1978 *Elements of X-ray diffraction* (Boston: Addison Wesley) p. 99

Devan R S, Kolekar Y D and Chougule B K 2008 *J. Alloys Compd.* **461** 678

Dong S, Li I F and Viehland D 2003 *IEEE Trans. Ultra. Ferro. Freq. Cont.* **50** 1253

Duong G V, Groessinger R and Turtelli R S 2006 *IEEE Trans. Magn.* **42** 3611

Eerenstein W, Mathur N D and Scott J F 2006 *Nature (London)* **442** 759

Fiebig M, Lottermoser T, Zrohlich D, Goltsev A V and Pisarev R V 2002 *Nature (London)* **419** 818

Fiebig M 2005 *J. Phys. D: Appl. Phys.* **38** R123

Fiebig M, Lottermoser T, Kneip M K and Bayer M 2006 *J. Appl. Phys.* **99** 08E302

Filipetti A and Hill N A 2001 *J. Magn. Magn. Mater.* **236** 176

Galt J K, Mathias B T and Remeika J P 1950 *Phys. Rev.* **79** 391

Gul I H, Ahmed W and Maqsood A 2008 *J. Magn. Magn. Mater.* **320** 270

Harnagea C, Mitoseriu L, Buscaglia V, Pallecchi I and Nanni V 2007 *J. Euro. Ceram. Soc.* **27** 3947

Jiang Q -H, Nan C -W and Shen Z -J 2006 *J. Am. Ceram. Soc.* **89** 2123

Jiang Q, Liu F, Yan H, Ning H, Libor Z, Zhang Q, Cain M and Reece M J 2011 *J. Am. Ceram. Soc.* **94** 2311

Kadam S L, Patankan K K, Mathe V L, Kothale M B, Kale R B and Chougule B K 2003 *Mater. Chem. Phys.* **78** 684

Kuroiwa Y, Aoyagi S, Sawada A, Harada J, Nishibori E, Takata M and Sakata M 2001 *Phys. Rev. Lett.* **87** 217601

Liu X -H, Xu Z, Wei X -Y, Dai Z -H and Yao X 2010 *J. Am. Ceram. Soc.* **93** 2975

Mandal A, Banerjee S, Banerjee S and Chakravorty D 2012 *J. Appl. Phys.* **112** 074310

Martinez B, Roig A, Obradors X, Molins E, Rouanet A and Monty C 1996 *J. Appl. Phys.* **79** 2580

Nersessian N, Wing S and Carman G 2004 *IEEE Trans. Magn.* **40** 71

Pal M, Brahma P, Chakravorty D, Bhattacharyya D and Maiti H S 1996 *J. Magn. Magn. Mater.* **164** 256

Parish M M and Littlewood P B 2008 *Phys. Rev. Lett.* **101** 166602

Raidongia K, Nag A, Sunderesan A and Rao C N R 2010 *Appl. Phys. Lett.* **97** 062904

Shen X, Zhou Z, Song F and Meng X 2010 *J. Sol–Gel Sci. Technol.* **53** 405

Smit J and Wijn H P J 1959 *Ferrites* (New York: Wiley), p. 221

Spaldin N A and Fiebig M 2005 *Science* **309** 391

Sreenivasulu G, Babu V H, Markandeyulu G and Murty B S 2009 *Appl. Phys. Lett.* **94** 112902

Srinivasan G, Rasmussen E T and Hayes R 2003 *Phys. Rev.* **B67** 014418

Tan S Y, Shannigrahi S R, Tan S H and Tay F E H 2008 *J. Appl. Phys.* **103** 094105

Testino A, Mitoseriu L, Buscaglia V, Buscaglia M T, Pallecchi I, Albuquerque A S, Calzona V, Marré D, Siri A S and Nanni P 2006 *J. Euro. Ceram. Soc.* **26** 3031

Uchino K, Sadanaga E and Hirose T 1989 *J. Am. Ceram. Soc.* **72** 1555

Yager W A, Merritt F R and Guillaud C 1951 *Phys. Rev.* **81** 477

Zhai J, Cai N, Shi Z, Lin Y and Nan C 2004 *J. Phys. D: Appl. Phys.* **37** 823

Zhao Z, Buscaglia V, Viviani M, Buscaglia M T, Mitoseriu L, Testino A, Nygren M, Johnsson M and Nanni P 2004 *Phys. Rev.* **B70** 024107

Zhang H F, Or S W and Chan H L W 2009 *Mater. Res. Bull.* **44** 1339

Zheng H *et al* 2004 *Science* **303** 661

Zhong W L, Wang Y G, Zhang P L and Qu B D 1994 *Phys. Rev.* **B50** 698